Direct Evidence of Hole Injection
Enhanced by O_2 Plasma Treatment on Indium Tin Oxide

Soo Young Kim and Jong-Lam Lee*

Department of Materials Science and Engineering, Pohang University of Science
and Technology (POSTECH), Pohang, Gyeongbuk 790-784, Korea

We have investigated interface dipole energies and the energy alignment between 4,4'-bis[N-(1-naphtyl)-N-phenyl-amino]biphenyl (α-NPD) and bare indium tin oxide (*ITO*)/O_2-plasma-treated ITO (*O_2-ITO*) anodes using synchrotron radiation photoemission spectroscopy (SRPES). SRPES spectra showed that the work function of *O_2-ITO* is 0.6 eV higher than that of *ITO*. After deposition of α-NPD, the dipole energy and amount of band bending were calculated to be - 0.1 and - 0.5 eV for *ITO* and - 0.3 and - 0.3 for *O_2-ITO*, respectively. It is thereupon concluded that the work function of *O_2-ITO* is still 0.6 eV higher than that of *ITO*, resulting in a decrease of the turn-on voltage *via* reduction of the hole injection barrier.

Keywords: organic light emitting diodes, hole injection barrier, x-ray photoemission spectroscopy, O_2 plasma treatment, indium tin oxide

1. INTRODUCTION

Organic light emitting diodes (OLEDs) have received considerable attention in recent years because of their scientific and commercial significance. One of the most important factors determining device function and performance is charge carrier injection from electrodes into the organic material. According to the vacuum level alignment rule, hole injection barriers are defined by the difference between the ionization energy of the organic material and the metal work function. In OLEDs, indium tin oxide (ITO) is widely used as a hole-injection electrode due to its high work function (~ 4.7 eV)[1]. In order to increase the work function of ITO, several kinds of surface treatment have been extensively studied in recent years[2,3]. A number of surface treatment methods were applied to the surface of ITO, such as mechanical polishing, plasma, and UV-ozone treatment. However, numerous photoelectron studies and Kelvin probe measurements have demonstrated that interface dipoles (Δ) can appear at the interface of metal with organic materials and affect the charge injection barrier[4]. It was reported that Δ originates from the charge transfer across the interface, redistribution of electron cloud, interfacial chemical reaction, or other types of electronic charge rearrangement[5]. Therefore, it is essential to understand the formation of the interface dipole between ITO and organic materials.

In this letter, we investigated the formation of an interface dipole between oxygen plasma-treated ITO (*O_2-ITO*) anode and 4,4'-bis[N-(1-naphtyl)-N-phenyl-amino]biphenyl (α-NPD). Synchrotron radiation photoemission spectroscopy (SRPES) was employed to observe the change of the energy level with *in situ* deposition of a α-NPD layer on an *O_2-ITO* anode. Based on these observations, the formation of an interface dipole between *O_2-ITO* and α-NPD in OLED is discussed.

2. EXPERIMENTAL PROCEDURE

A glass coating with ITO (150 nm thick, ~ 20 $\Omega/\square$) was used as the starting substrate. The ITO surface was cleaned in sequence with acetone, iso-propyl alcohol, and deionized water, and then dried with high purity nitrogen gas. The ITO surface was treated with O_2 plasma for 1 min with a power of 150 W. For reference, ITO without plasma treatment (*ITO*) was also prepared. Two samples were loaded into a thermal evaporator and α-NPD with a thickness of 70 nm, tris (8-hydroxyquinoline) aluminum (Alq_3, 60 nm), and aluminum (Al, 150 nm) layers were deposited in sequence. During the deposition, the base pressure of the chamber was maintained as low as 10^{-6} Torr. The active area of the device was 3×3 mm^2. The current density-voltage characteristics of the devices were measured.

For the measurement of SRPES spectra, *O_2-ITO* and *ITO*

*Corresponding author: jllee@postech.ac.kr

samples were loaded into a vacuum chamber equipped with an electron analyzer at the Pohang Accelerator Laboratory 2B1 beam line. α-NPD was then deposited *in situ* on the samples using a thermal evaporator. The evaporation of α-NPD was performed in a separately connected preparation chamber and core level spectra were obtained in the main chamber using an incident photon energy of 600 eV. In order to exclude the photovoltaic effect, samples were kept in darkness during photoemission measurements. The α-NPD coverage at each step was determined by comparing the atomic ratio of C 1s over In 3d. At each step, the sample was characterized by measuring the valence band spectra, the core level spectra, and the secondary electron emission spectra. The changes in core level binding energy indicate band bending and secondary electron emission spectra give the change in work function. Here, following the convention in surface science, the change of work function is considered as positive when the vacuum level is raised by deposition. Therefore, the dipole energies are calculated by the sum of band bending and change of work function. The onset of photoemission was measured with a negative bias (-20 V) on the sample so as to avoid the work function of the detector. The incident photon energy was calibrated with the core level spectrum of Au 4f.

3. RESULTS AND DISCUSSION

Figure 1 shows the current density-voltage characteristics of the two devices. The operation voltage at the current density of 100 mA/cm^2 of OLEDs using O_2-*ITO* decreased from 34 V to 14 V. The decrease in operation voltage is a reflection of improved hole injection efficiency. Luminance-voltage curves are shown in Fig. 1(b). The operation voltage corresponding to 500 cd/m^2 was 13 V for O_2-*ITO* and 35 V for *ITO*, respectively. The optical image at a luminance of 500 cd/m^2 is shown in the inset of Fig. 1(b). It is thought that holes were effectively injected from the anode to the organic layer, promoting internal quantum efficiency.

Figure 2 shows the change of C 1s SRPES spectra according to the deposition steps of α-NPD on (a) *ITO* and (b) O_2-*ITO*. The molecular structure of α-NPD is shown in the inset of Fig. 2(a). In order to separate the chemical bonding states included in the spectra, the spectral line shape was simulated using an asymmetric Gaussian-Lorentzian sum function. We used an 80% Gaussian function and a 20% Lorentzian function to fit the sum of the separation peaks to the original peaks. Shirley background subtraction was used to minimize the background effects of C 1s spectra. The C 1s peak was separated into two components. The bulk component of C-O and the surface component of C-C were considered. The binding energy of the C-O bond was higher than that of the C-C binding energy, which agrees well with a previously reported value[6]. In the as-deposited state, C 1s peaks are
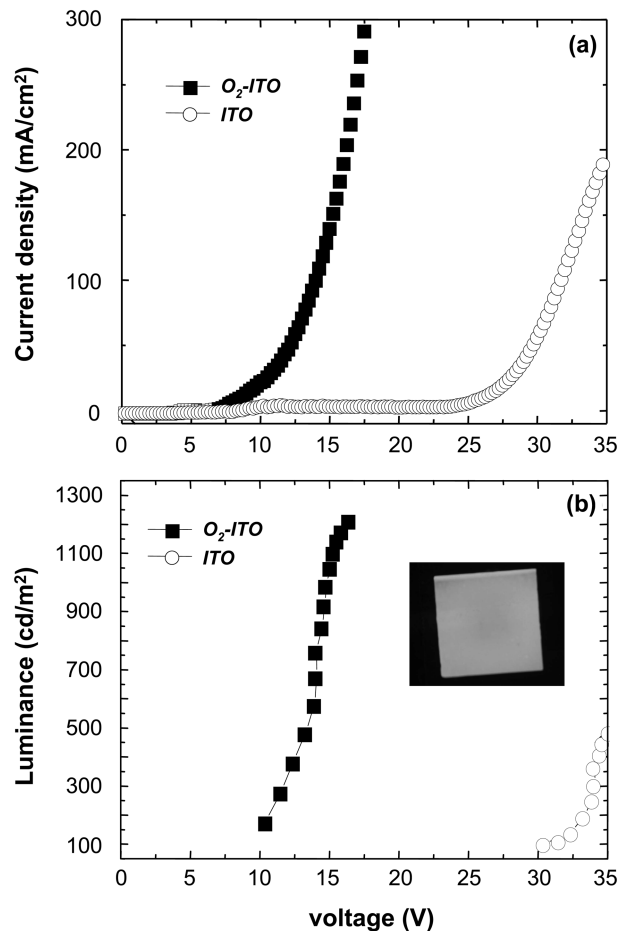

Fig. 1. (a) Current density-voltage characteristics of OLEDs with different anodes.
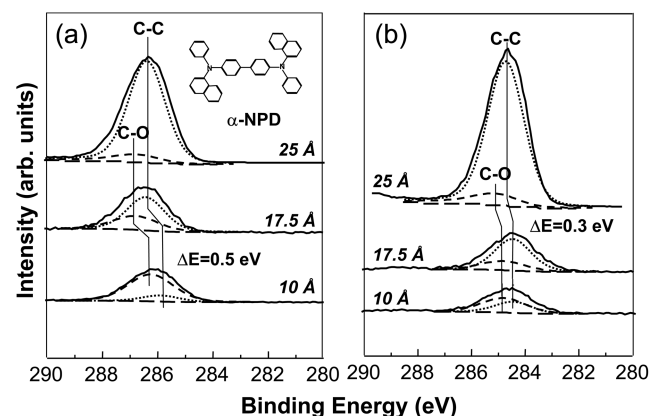

Fig. 2. C 1s core level spectra for (a) *ITO* and (b) O_2-*ITO*.

wholly composed of C-O bonds. According to the deposition of α-NPD on both samples, the peak corresponding to the C-C bond shifted about 0.5 eV in *ITO* and 0.3 eV in O_2-*ITO* toward high binding energy and the peak intensity increased due to the composition of α-NPD. These results demonstrate that the amount of downward band bending in
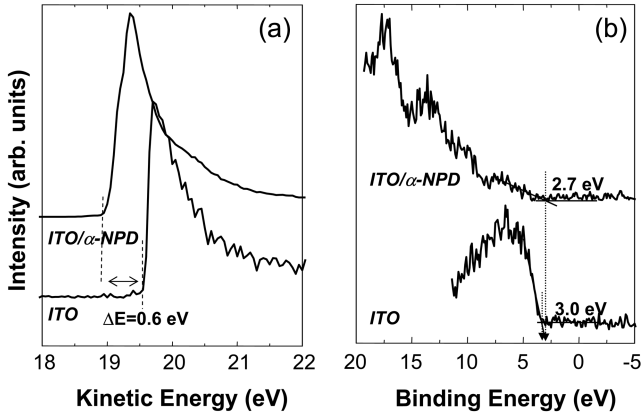
Fig. 3. (a) Secondary electron emission spectra and (b) valence band spectra for *ITO*.

Fig. 4. (a) Secondary electron-emission spectra and (b) valence band spectra for *O₂-ITO*.

ITO is higher than that in *O₂-ITO*.

In order to clarify the change of work function with deposition of α-NPD on *ITO*, the SRPES spectra of secondary electron were measured, as shown in Fig. 3(a). The onset of a secondary electron peak shifted toward lower kinetic energy by 0.6 eV after deposition of α-NPD, indicating a decrease in the work function. Figure 3(b) shows the change of valence band spectra with deposition of α-NPD. The onset of the valence band maximum (VBM) was determined by extrapolating two solid lines from the background and straight onset in the spectra[7]. Before deposition of α-NPD, the VBM was located at 3.0 eV, indicating that the energy difference between VBM of *ITO* and Fermi level (E_F) is 3.0 eV. After deposition of α-NPD, the VBM was located at 2.7 eV, meaning that the energy difference between the highest occupied molecular orbital (HOMO) and E_F of α-NPD on *ITO* is 2.7 eV. This in turn indicates that the hole injection barrier from *ITO* to α-NPD is 2.7 eV.

Figure 4(a) shows the change of work function with deposition of α-NPD on *O₂-ITO*. The onset of the secondary electron peak shifted about 0.6 eV toward lower kinetic energy after deposition of α-NPD, reflecting a decrease in the work function. The change of VBM with deposition of α-NPD is shown in Fig. 4(b). Before deposition of α-NPD on *O₂-ITO*, the VBM was located at 2.5 eV. After deposition of α-NPD, the VBM was located at 2.1 eV, meaning that the HOMO level of α-NPD is located 2.1 eV apart from E_F. This result indicates that the hole injection barrier from *O₂-ITO* to α-NPD is 2.1 eV.

Based on these experimental observations, the formation of an interface dipole on ITO can be explained as follows. As the thickness of α-NPD on *ITO* increases, the core level peaks shift to the higher binding energy by about 0.5 eV [Fig. 2(a)], indicating downward band bending in α-NPD along the interface to the surface. The onset of secondary emission in *ITO* shifted to lower kinetic energy by about 0.6 eV with deposition of α-NPD [Fig. 3(a)], indicating a
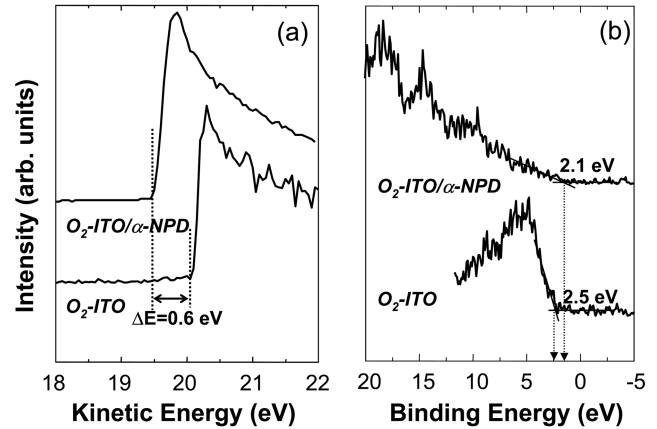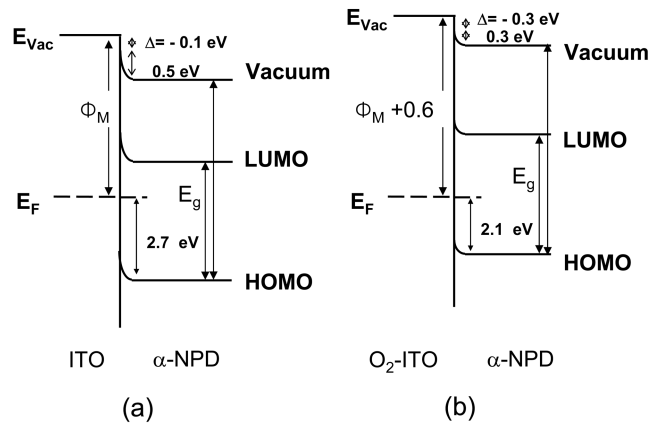

Fig. 5. Schematic band diagram: (a) *ITO* and (b) *O₂-ITO*.

decrease in the work function on the surface of α-NPD. Considering the band bending of 0.5 eV toward the α-NPD, Δ is determined to be - 0.1 eV, as shown in Fig. 5(a). Figure 5(b) shows a schematic band diagram for the deposition of α-NPD on the *O₂-ITO* anode. The work function of *O₂-ITO* is 0.6 eV higher than that of *ITO*, as shown in Figs. 3(a) and 4(a). The amount of band bending and the change of work function with deposition of α-NPD are 0.3 eV [Fig. 2(b)] and 0.6 eV [Fig. 4(a)], respectively. Thus, the value of Δ produced at the interface of *O₂-ITO* with α-NPD corresponds to - 0.3 eV, as shown in Fig. 5(b). It was previously reported that as the work function of a metal substrate becomes higher, Δ also increases due to increased sensitivity in the electron density tail[8]. In a metal-organic system, the metal work function changes with the surface-dipole, which originates from the tail of free electrons[9]. The contribution of the surface-dipole could be modified by the presence of an adsorbate. ITO has metallic properties, preserving many free electrons. As a result, Δ in *O₂-ITO* is higher than Δ in *ITO*. However, the amount of band bending in *O₂-ITO* is lower

than that in *ITO*, as shown in Fig. 2, indicating a smaller space charge region in *O₂-ITO*. Therefore, O_2 plasma treatment increased the work function of the electrode and reduced the space charge region between the electrode and the organic material, leading to a decrease in the hole injection barrier from 2.7 to 2.1 eV. Therefore, the operation voltage at the current density of 100 mA/cm² of OLEDs using *O₂-ITO* decreased from 34 V to 14 V.

4. CONCLUSION

In conclusion, we investigated the formation of an interface dipole between an *O₂-ITO* anode and α-NPD. The operation voltage at the current density of 100 mA/cm² of OLEDs using *O₂-ITO* drastically decreased from 34 V to 14 V. SRPES spectra showed that the dipole energies of *ITO* and *O₂-ITO* are - 0.1 and - 0.3 eV, respectively. The amount of band bending in *O₂-ITO* is 0.2 eV lower than that in *ITO*, indicating a smaller space charge region in *O₂-ITO*. The work function of α-NPD on *O₂-ITO* is 0.6 eV higher than that of *ITO*. Thus, O_2 plasma treatment on ITO lowers the potential barrier for hole injection from ITO to α-NPD, thereby reducing the turn-on voltage of OLEDs.

ACKNOWLEDGEMENTS

REFERENCES

1. T. Sano, Y. Hamada, and K. Shibata, *IEEE J. Selected Top. Quantum Electron*. **4**, 34 (1998).
2. K. Sugiyama, H. Ishii, Y. Ouchi, and K. Seki, *J. Appl. Phys*. **87**, 295 (2000).
3. C. Donley, D. Dunphy, D. Paine, C. Carter, K. Nebesny, P. Lee, D. Alloway, and N. R. Armstrong, *Langmuir* **18**, 450 (2002).
4. N. Koch, A. Kahn, J. Ghijsen, J.-J. Pireaux, J. Schwartz, R. L. Johnson, and A. Elschner, *Appl. Phys. Lett.* **82**, 70 (2003).
5. H. Ishii, K. Sugiyama, E. Ito, and K. Seki, *Adv. Mater.* **11**, 605 (1999).
6. J. F. Moulder, W. F. Strickle, P. E. Sobol, and K. D. Bomben, *Handbook of X-ray Photoelectron Spectroscopy*, p. 41, Perkin-Elmer, Eden Prairie, Minesota (1992).
7. J. M. Baik and J.-L. Lee, *Met. Mater. Int.* **10**, 555 (2004).
8. I. G. Hill, A. Rajagopal, A. Kahn, and Y. Hu, *Appl. Phys. Lett.* **73**, 662 (1998).
9. X. Crispin, V. Geskin, A. Crispin, J. Cornil, R. Lazzaroni, W. R. Salaneck, and J.-L. Brédas, *J. Am. Chem. Soc.* **124**, 8131 (2002).